First Result of Field Extrapolation Based on HMI Vector Magnetic Data

Xudong Sun[1], Todd Hoeksema[1], Thomas Wiegelmann[2], Yang Liu[1], Keiji Hayashi[1]

[1.] HEPL, Stanford University; [2.] MPI, Germany (contact: *xudongs@stanford.edu*)

Abstract

• The Helioseismic and Magnetic Imager (*HMI*) provides high resolution, high cadence full disk vector magnetograms.

• The HMI pipeline inverts Stokes vector near real time, fully disambiguates azimuth, detects and provides vector patches in various coordinates.

• We have implemented various extrapolation models in the pipe-line. Some quick-look products will be provided routinely.

• We report the first result using the non-linear force-free field (*NLFFF*) extrapolation [*Wiegelmann, 2004*] to study two active regions with *HMI* vector magnetic data.

Method

• Data inverted using *VFISV* [*Borrero, 2010*], disambiguated using a minimum energy method [*Metcalf, 1994; Leka, 2009*]. Active region is auto-identified [*Turmon, 2010*].

• We use a *NLFFF* code based on optimization method with pre-processed boundary condition [*Wiegelmann, 2004, 2008*].

• Performed on a ~0.5 arcsec resolution and ~12 min cadence.

SDO 'First Light' Event (AR11060, Apr 8th)

• B-3 two-ribbon flare (*fig 2*), CME, global EUV disturbance [*Liu et al., 2010*].

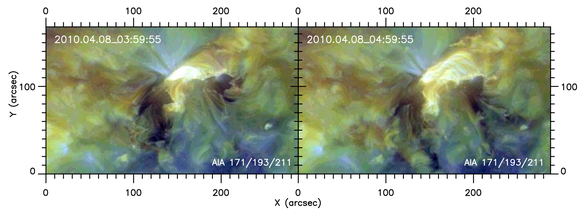

Fig 1: AIA 171/193/211 composite image of the event at 0400UT and 0500UT of April 8th . Lower loops brightened up after the flare; higher loops brightened ~1hr later (courtesy C. Shrijver).

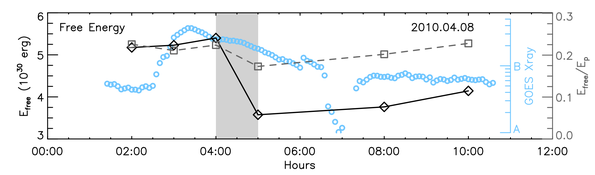

Fig 2: Solid line: free magnetic energy evolution as derived from NLFFF model. Dashed line: ratio of free energy to potential field energy. Blue circles: GOES 5min soft X-ray flux.

• No drastic change is found in photospheric field.

• *NLFFF* extrapolation estimates free magnetic energy on the order of 10^{30} erg, ~20% of the minimal potential field energy (*fig 2*).

• Higher loops starts to brighten ~1 hr after the flare (*fig 1*).

• A ~40% drop in free energy is seen between 0400UT and 0500UT (*fig 2*), after the higher loops starts to brighten up.

Confined Flare (AR11117, Oct 25th)

• Fast evolving AR with flux emergence between 21st and 29th. A confined C-2 flare (*fig 6, 7a*) happened around 2210UT on 25th.

• Coronal loops roughly match potential field. A net negative flux is seen (*fig 5*). *AIA* images confirm large scale loop connectivity to nearby positive flux (*fig 7a*).

• A small pair of flux emerges at center carries strong current (*fig 3, 7d*). Shear along polarity inversion line (PIL) is ~45° with a gradual decrease in time (*fig 4*).

• Total energy is on the order of 10^{32} erg and keeps increasing as new flux brings in energy (*fig 7f*), despite repeating small flares.

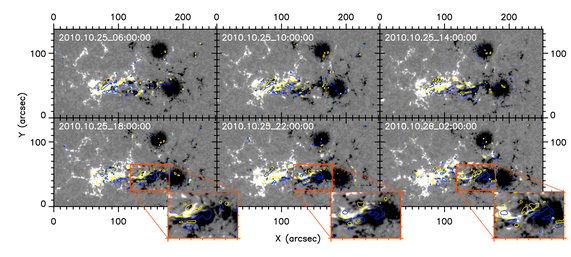

Fig 3: (top right) 6 frames of vertical magnetic field Bz for AR11117 shown in gray scale, color saturated at 500G. Each frame is 6 hours apart. Yellow and purple lines are contours of vertical current Jz at 5 σ level. Red boxes in the lower row contain the pair of emerging flux with high current.

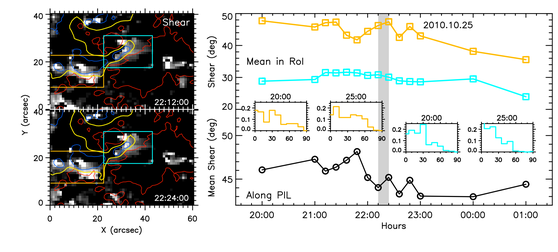

Fig 4: (lower right) Left: Shear angle show in the b/w background for the same cutout region as in lower row of fig 3, for 2212UT and 2224UT during the flare. White color indicates high shear. Blue and red contours are for Bz over 300G. Yellow lines is the polarity inversion line (PIL). Orange and cyan boxes show two regions with high shear. Upper right: Mean shear angle evolution for two regions of interest (RoI). 4 histograms show the shear angle distribution within two boxes at 2000UT and 2500UT. Lower right: mean shear along PIL within the boxes.

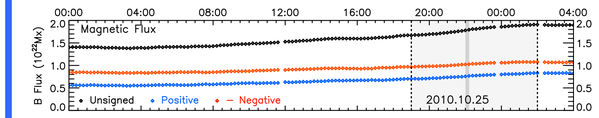

Fig 5: Vertical magnetic flux computed from vector data for October 25th. Black is the unsigned flux. Blue/Red are the positive/ negative flux. Light gray indicates the period covered in this study. Dark gray is when the flare takes place.

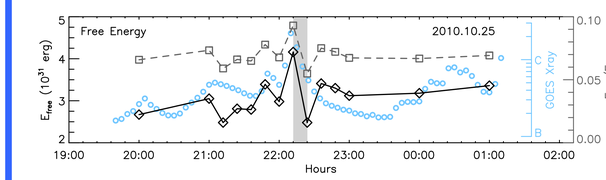

Fig 6: Same as fig 2, for AR11117 on October 25th.

• NLFFF extrapolation estimates free energy on the order of 10^{31} erg, ~5% of the potential field energy. A ~30% drop in free energy is found right after the flare (*fig 6*).

• Complex field topology is modeled and is seen from the low-lying loops in AIA image (*fig 7abe*).

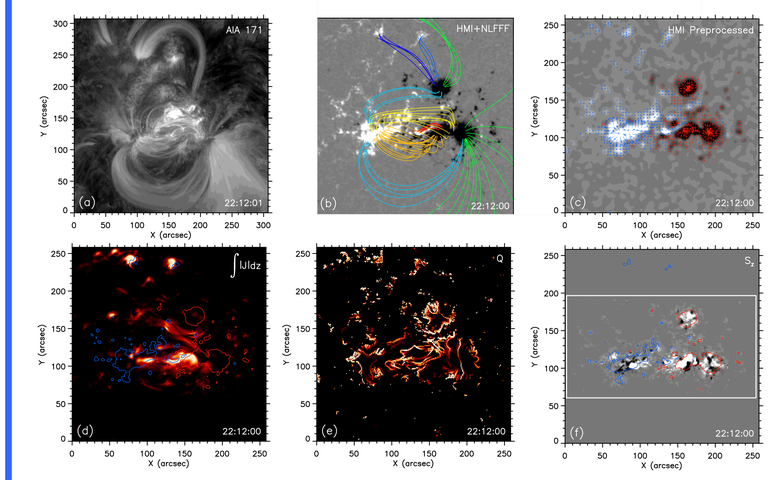

Fig 7: (a) AIA 171 image at onset of flare. (b) Top down view of selected field lines from NLFFF extrapolation. Different colors show different connectivity of the lines. Some green 'open' lines close outside the domain. Red shows the current carrying lines. (c) Pre-processed HMI vector data [Wiegelmann et al., 2008] as boundary condition. (d) Background shows total current density integrated over height [DeRosa et al., 2009]. Blue/Red contours are for Bz at 300G. (e) Q from extrapolation as a proxy for quasi-separatrix layers (QSL) of field topology [Titov et al., 2002]. Pixels with |B| below 100G are filtered out. (f) Vertical component of Poynting vector computed from the DAVE4VM model [Schuck, 2008]. White shows energy influx (implemented in HMI pipeline; courtesy P. Schuck).

Conclusions and Future Work

• Free energy drop is found in *preliminary* analysis for both events after the flare. Significance of result is yet to be determined.

• Optimization of model parameters is needed. *NLFFF* code in spherical coordinates may help study larger regions.

• Larger number of events is needed to establish statistical trends.

• Borrero, J. M. et al., 2010, *Solar Phys.*, arXiv:0901-2702.
• DeRosa, M. et al., 2009, *ApJ.*, **696**, 1780.
• Leka, K. D. et al., 2009, *Solar Phys.*, **260**, 83.
• Liu, W. et al., 2010, *ApJL.*, **723**, L53.
• Metcalf, T. R., 1994, *Solar Phys.*, **155**, 235.
• Schuck, P. W., 2008, *ApJ.*, **683**, 1134.
• Titov, V. et al., 2002, *JGR.*, **107**, 3.
• Turmon, M. et al., 2010, *Solar Phys.*, **262**, 277.
• Wiegelmann, T., 2004, *Solar Phys.*, **219**, 87.
• Wiegelmann, T. et al., 2008, *Solar Phys.*, **247**, 249.